Geophys. J. Int. (2000) **141,** 337–350

Palaeomagnetic results from remagnetized mid-Cretaceous (Albian–Cenomanian) strata of northeastern Venezuela

V. Costanzo-Alvarez,[1] W. Williams,[2] A. Pilloud,[3] O. Mirón[4,*] and M. Aldana[1]

[1] *Departamento de Ciencias de la Tierra, Universidad Simón Bolívar, Sartenejas, Baruta, Edo. Miranda, Venezuela*
[2] *Department of Geology and Geophysics, University of Edinburgh, West Mains Road, Edinburgh,* EH9 3JW, *UK. E-mail: wyn.williams@ed.ac.uk*
[3] *INTEVEP S.A., Departamento de Ciencias de la Tierra, Apdo.* 76343, *Caracas* 1070 A, *Venezuela*
[4] *BP Exploration Venezuela, Centro Seguros SudAmerica, El Rosal, Caracas, Venezuela*

Accepted 1999 November 22. Received 1999 November 22; in original form 1999 June 8

SUMMARY

We report palaeomagnetic and rock magnetic results of a sedimentary sequence (Pertigalete cement quarry) located in northeastern Venezuela. Sampling was restricted to the vicinity of the contact between the upper Cretaceous Chimana and Querecual formations. Biostratigraphic evidence reveals an upper Albian age for this formational transition. Profiles of site-averaged NRM intensity of the high-coercivity (over 30 mT) and high-temperature (over 400 °C) components appear to be related to the contact and distance from the contact. We interpret this profile as the probable outcome of overlapping thermochemical remagnetization events resulting from hydrothermal activity that was focused along the two formations. Direct spectral analyses performed on the site-averaged stable NRM intensity profile allow the separation of at least two of these remagnetization events. On the other hand, palaeomagnetic results show a considerable streaking of site mean declinations, suggesting that tectonic or structural horizontal movements around a vertical axis have occurred after NRM acquisitions. Horizontal rotation angles, plotted against stratigraphic levels for bedding-corrected data, show some features that seem to coincide with the alteration peaks isolated in the profile of site-averaged stable NRM intensities. Thus, it appears that repeated thermochemical remagnetizations with overlapping unblocking spectra, and horizontal movements around a vertical axis could have been responsible for much of the within-site dispersion. A simple three-stage reconstruction of the possible chain of thermochemical and tectonic occurrences that could lead to the present-day palaeomagnetic and rock magnetic evidence is proposed. These events, including clockwise horizontal rotations around a vertical axis, are tentatively placed in a geological time framework between middle Miocene and Pliocene times according to the main geological and geochemical evidence available.

Key words: Cretaceous, chemical remanent magnetization, palaeomagnetism, rock magnetism, spectral analysis, transition zone.

INTRODUCTION

Palaeomagnetic evidence for horizontal rotations (around a vertical axis) of Palaeozoic and Mesozoic units in northern Venezuela and the nearby Caribbean islands has been documented in the literature (e.g. MacDonald & Van Horn 1977; Skerlec & Hargraves 1980; MacDonald 1980; Stearns *et al.* 1982; Maze & Hargraves 1984; Duncan & Hargraves 1984; Perarnau 1985; MacDonald 1990; Burmester *et al.* 1996). One of the chief concerns in most of these works is to determine the timing when rotations took place. Many of these studies (e.g. Skerlec & Hargraves 1980; Stearns *et al.* 1982) have been performed on intrusive igneous or metamorphic rocks for which an age of magnetization is difficult to establish. Comparing coeval palaeomagnetic poles is not a viable way of dating these rotations since there is not yet a reliable apparent polar wander path for the Caribbean Plate. Sometimes secondary magnetizations are not easily distinguished from their primary counterparts because of similarities of Mesozoic directions to that of the present geomagnetic field, thus adding more uncertainties to the timing of NRM acquisitions and tectonic or structural rotations.

* Now at: Department of Geology and Geophysics, University of Edinburgh, West Mains Road, Edinburgh, EH9 3JW, UK.

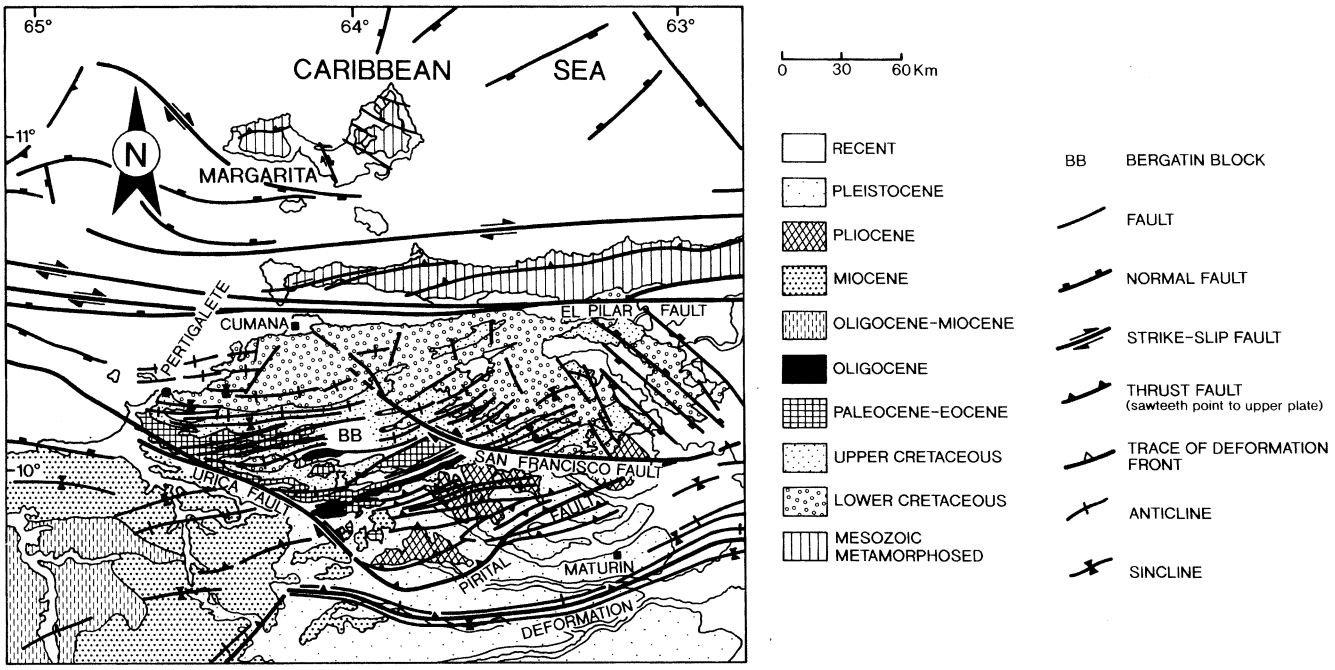

Figure 1. Geological map of the Pertigalete area showing the main structural features.

In this study we attempt to establish time constraints for some of these horizontal movements using a rather different approach. Our primary objective is to isolate the main alteration events that have affected a sedimentary sequence and that are most probably related to various remagnetization events. Providing we can establish a sequence of relative ages for these events, associated with rotated and non-rotated NRMs, it should also be possible to determine an age bracket for their occurrences in the geodynamic framework of northeastern Venezuela. Late remagnetizations are used here in order to constrain the timing of rotations of the magnetic overprints.

The sedimentary sequence we have studied is located at the Pertigalete cement quarry (upper Cretaceous) within the Bergantín block in northeastern Venezuela (Fig. 1). Passalacqua *et al.* (1995) have previously addressed the problem of quantification of the structural rotations in this specific block and the need for palaeomagnetic constraints. Our sampling has been performed in four different localities at the remagnetized strata adjacent to the contact between the Chimana and Querecual formations (Fig. 2). It has been pointed out, by combined rock magnetic and dielectric characterizations of Chimana and Querecual rocks (Suárez *et al.* 1999 and Costanzo *et al.* 1999), that such a lithological transition might have acted as a focus of alteration upon its contiguous sedimentary horizons. Palaeomagnetic and rock magnetic results (that is, analyses of IRM acquisition and composite IRM thermal demagnetization curves) are complemented by some biostratigraphic analyses of foraminifera in order to characterize the Chimana/Querecual lithological contact better.

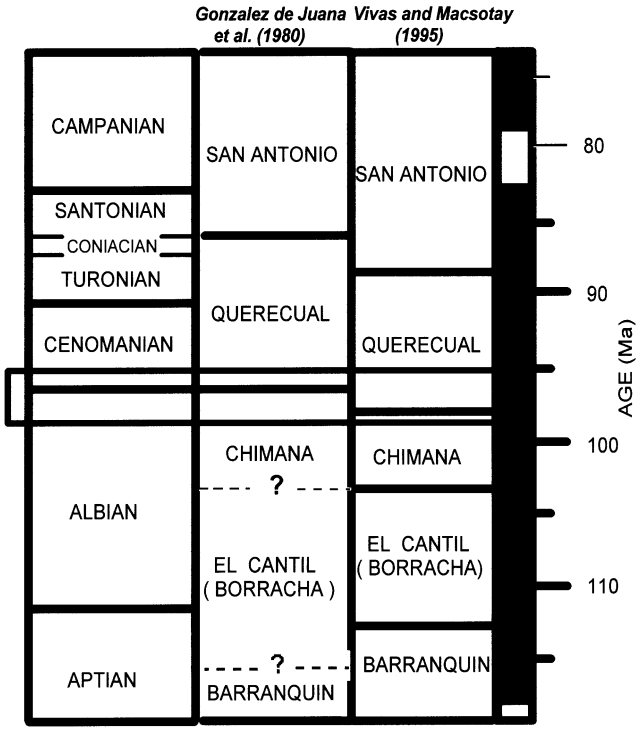

Figure 2. Middle to upper Cretaceous stratigraphic column of the Pertigalete sequence (Gonzalez de Juana *et al.* 1980; Vivas & Macsotay 1995) compared to the geomagnetic reversal timescale (Harland *et al.* 1992). The approximate range of sedimentary horizons sampled for this study around the Chimana/Querecual contact is indicated by the double bars.

GEOLOGICAL SETTING, BIOSTRATIGRAPHY AND PALAEOMAGNETIC SAMPLING

For this study we have collected, in the Pertigalete cement quarry (northeastern Venezuela), an average of eight oriented samples (drilling cores) per sedimentary horizon. The sampling was performed in four different localities or outcrops separated by distances of no more than 500 m (i.e. Querecual QL1-4 and Chimana CL1-4). Each sampled horizon is considered here

as a site and in most cases a maximum vertical distance of approximately 5 m separates two adjacent sites (24 horizons: 167 specimens).

All the Cretaceous sequences in northern Venezuela (e.g. Pertigalete) were deposited in a passive margin as a response to subsidence and worldwide eustatic sea-level changes. At present, the region where Pertigalete is located (Bergantín block) appears to be entirely folded and faulted, mainly because of the interaction between the South American and Caribbean plates. Consequently, deformation features in the region show W–E- and SW–NE-trending strikes as vestiges of clockwise tectonic rotations (Fig. 1). The Pertigalete quarry is flanked by the Urica and San Francisco faults, which have been interpreted, on purely seismic grounds, as lateral ramps of the Pirital thrust (Passalacqua *et al.* 1995). The movement of these faults could have accounted for some small anticlockwise movements as well.

Since our palaeomagnetic sampling took place in a still active cement quarry we had easy access to good rock exposures and to a fair structural control on the sampling sites. All the outcrops appear to be part of a major fold with bedding surfaces dipping progressively from southeastwards (Chimana most distant sites) to northeastwards (Chimana and Querecual sites around the Chimana/Querecual transition) at angles that range from 19° up to 83°.

In the Pertigalete sequence, Chimana sediments form 20–40 m thick layers of yellow to light red sandstones and siltstones typical of a coastal or inner neritic depositional palaeoenvironment (coarse-grained and moderately sorted sediments). Querecual rocks, however, appear as dark grey limestones that have been deposited in an anoxic palaeoenvironment. They also exhibit some lamination and a light foetid smell.

Chimana lithologies change, over a vertical distance of approximately 6 m, to the micritic limestones of the Querecual formation. The Chimana/Querecual contact is easily distinguishable in the field by the presence of numerous calcite veins and a progressive change of colour in the transitional Chimana lithologies, accompanied by a decrease of mineral grain sizes and a diminution of the content of detritic quartz. Chemical analyses (Suárez *et al.* 1999) also show marked changes in $H2O^-$, SiO_2 and CO_2 content throughout this lithological transition.

Visual analysis of Querecual rocks reveals a range of contrasting appearances that seems to be linked to both alteration and distance from the contact. In fact, yellowish-brown stained limestones with some reddish mottling are characteristic of those horizons that lie close to the Chimana/Querecual contact, whereas mainly homogeneous (apparently fresh) dark grey rocks appear at the most distant sites. Querecual rocks were sampled more extensively than the Chimana rocks due to the high degree of recent weathering shown by the latter, which not only forecast poor palaeomagnetic behaviour but also made their sampling extremely difficult due to their crumbling texture.

The Chimana/Querecual contact roughly coincides with the Albian/Cenomanian time boundary (Gonzalez de Juana *et al.* 1980) (Fig. 2). More recently, Vivas & Macsotay (1995) have assigned to the bottom of Querecual (just above the contact with Chimana) a slightly older age, within the biozones of the planktonic foraminifera *Rotalipora ticinenses* and *Rotalipora appeninica* (upper Albian) (Fig. 2).

In order to characterize the Querecual lithologies better, eight samples from the collection (i.e. sites QL3-1, QL1-1, QL4-1, QL3-2, QL3-4, QL2-2, QL2-3 QL2-4) were used for biostratigraphic purposes (planktonic foraminifera). The faunal associations observed are representative of the Querecual formation. However, apart from samples QL1-1 and QL4-1, good planktonic markers were not identified. Although the absence of such markers does not allow us to refine the age constraints for these sediments, an important contrast of microfaunal associations was recognized. This contrast typifies two groups of samples, namely the interval QL3-1 to QL3-4 (0.5–7 m from the contact) with a mid- to upper Albian age, and QL2-2 to QL2-4 (16–23 m from the contact) with an upper Cenomanian age. Because of the restrictive presence of *Biticinella subbreggiensis* at sites QL1-1 and QL4-1, it can be argued that these two samples, located at 1.5 and 3.35 m, respectively, from the contact with Chimana, must have been deposited during late–mid-Albian/early upper Albian times. Thus, the Chimana/Querecual contact at the Pertigalete location is most likely to be upper Albian in age.

PALAEOMAGNETIC RESULTS

Demagnetization

Specimens were either stepwise demagnetized using alternating fields (AF) up to 60 mT, or thermally demagnetized, from 50 °C (at about 50 °C increments) up to about 700 °C. Remanence measurements were performed in a 2G Enterprises cryogenic magnetometer with a sensitivity of 10^{-11} A m^{-1}.

Figs 3, 4 and 5 show a few examples of Chimana and Querecual specimens (i.e. CL and QL) that have been AF and thermally demagnetized. Specimen CL2-2-4, located at −5 m below the contact (Fig. 3a), exhibits an NRM with unblocking temperatures (T_{UB}) higher than 600 °C. On the other hand, specimen CL2-3-5, at −8 m from the contact, has two overlapping NRMs indicated by linear segments in the vector demagnetization trajectories (Fig. 3b), namely a low-T_{UB} ($\sim$300 °C) component superimposed on a high-T_{UB} component (over 600 °C). Haematite seems to be an important NRM carrier in both Chimana specimens.

Querecual specimen QL1-1-6 (Fig. 4a), located at 1.5 m above the contact with Chimana, shows a steady decrease of the intensity of magnetization over the 20–60 mT range characteristic of fine-grained magnetite. Further thermal demagnetization with maximum T_{UB}s around 580 °C seems to confirm that fine-grained magnetite is the main NRM carrier in this specimen. QL3-1-4, at 0.5 m from the contact, appears to be univectorial (Fig. 4b) with an NRM carried by both magnetite (steady decrease of the NRM intensity up to 400 °C) and haematite (maximum T_{UB}s $\geq$ 600 °C).

QL1-2-2 (Fig. 5a) and QL3-5-6 (Fig. 5b), at 3.5 and 7.5 m from the contact, respectively, have overlapping components. In fact, the orthogonal projection for specimen QL1-2-2 shows that a soft easterly and shallow magnetization is partially removed in the range 200 °C $< T_{UB} <$ 400 °C to reveal an underlying harder remanence with a NE direction and T_{UB} as high as 600 °C. The rather smooth transition between two superimposed magnetizations in QL1-2-2 does not allow a complete separation of the overlapping NRMs, suggesting a thermochemical origin for at least the softer overprint (McClelland-Brown 1982). In the case of QL3-5-6 there is a

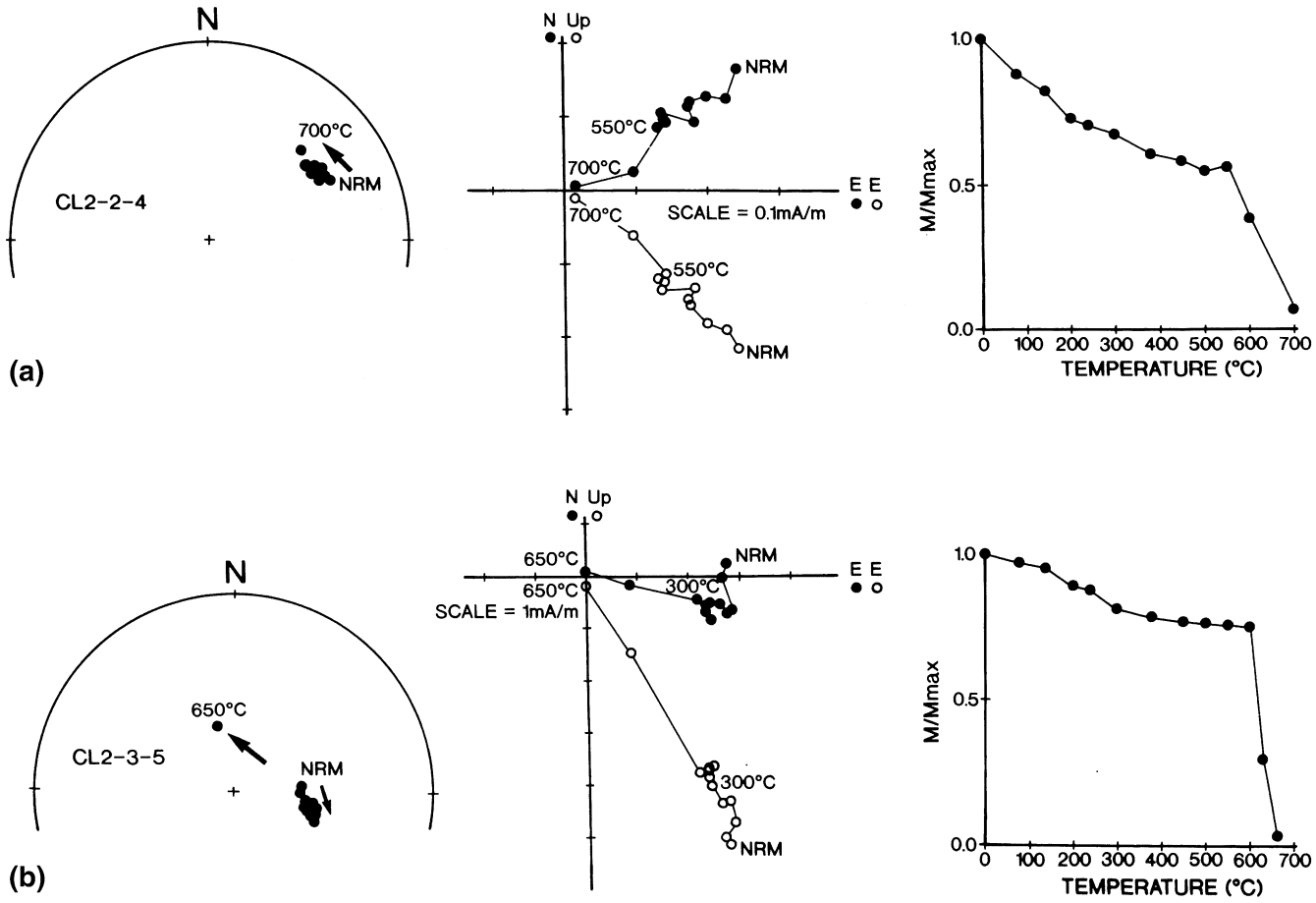

Figure 3. Orthogonal vector and equal-area projections of magnetization vectors (stratigraphic coordinates) for thermal demagnetization and the corresponding normalized intensity decay curves are shown for two representative specimens: (a) CL2-2-4 (Chimana formation, 5 m from the Chimana/Querecual contact) and (b) CL2-3-5 (Chimana formation, −8 m from the Chimana/Querecual contact). Specimens were stepwise demagnetized using alternating fields (AF) up to 60 mT or thermally demagnetized from 50 °C (at about 50 °C increments) up to about 700 °C.

third component in the hybrid transition between softer and harder components (10–60 mT). Orthogonal projections show that all the superimposed directions of remanence in this specimen should have similar W or SW declinations and shallow inclinations.

NRM carriers

In order to characterize the main NRM carriers we have also conducted analyses of IRM acquisition curves and thermal demagnetization of composite IRMs (Lowrie 1990) for some representative samples of our collection. Composite IRMs were induced by applying low, intermediate and high magnetic fields along three orthogonal directions (i.e. $X = 120$ mT, $Y = 400$ mT and $Z = 1000$ mT) of cylindrical (1.5 × 1.5 cm) rock samples. They were then stepwise thermally demagnetized, and the magnetizations measured along each of these axes for every single demagnetization step.

Fig. 6 shows some individual examples of IRM acquisition and composite IRM thermal demagnetization curves for two Chimana samples, CL2-3 and CL1-2, located at ∼−8 and −3.3 m, respectively, from the contact with Querecual. IRM acquisition curves for these two samples have a steep slope up to 200 mT and a more gradual increase at fields over 200 mT. This behaviour suggests the presence of high-coercivity haematite coexisting with a low-coercivity magnetic mineral (e.g. magnetite).

Thermal demagnetizations of composite IRMs reveal that the low- and intermediate-coercivity fractions of the IRMs (solid circles and triangles in Fig. 6) are dominant in these two samples. Although these IRMs have a moderate decay over a wide range of unblocking temperatures, they both show high unblocking temperatures (∼700 °C). However, the drop of NRM intensity of the IRMs at ∼700 °C, typical of haematite, appears to be more conspicuous in CL1-2 (Fig. 6b) than in CL2-3 (Fig. 6a).

Fig. 7 shows some individual examples of IRM acquisition and composite IRM thermal demagnetization curves for three Querecual samples, QL2-1, QL3-4 and QL3-2, located at ∼11.5, 7 and 4 m, respectively, from the contact with Chimana. In sample QL2-1 (Fig. 7a) most of the IRM is acquired prior to the 200 mT step, suggesting the dominance of a low-coercivity phase such as magnetite. However, this IRM does not reach complete saturation within the maximum applied field of 1000 mT due to the presence of some high-coercivity magnetic phases as well (i.e. haematite and goethite). Conversely, QL3-4 (Fig. 7b) shows complete saturation after a considerable initial increase at applied fields below 200 mT. On the other hand,

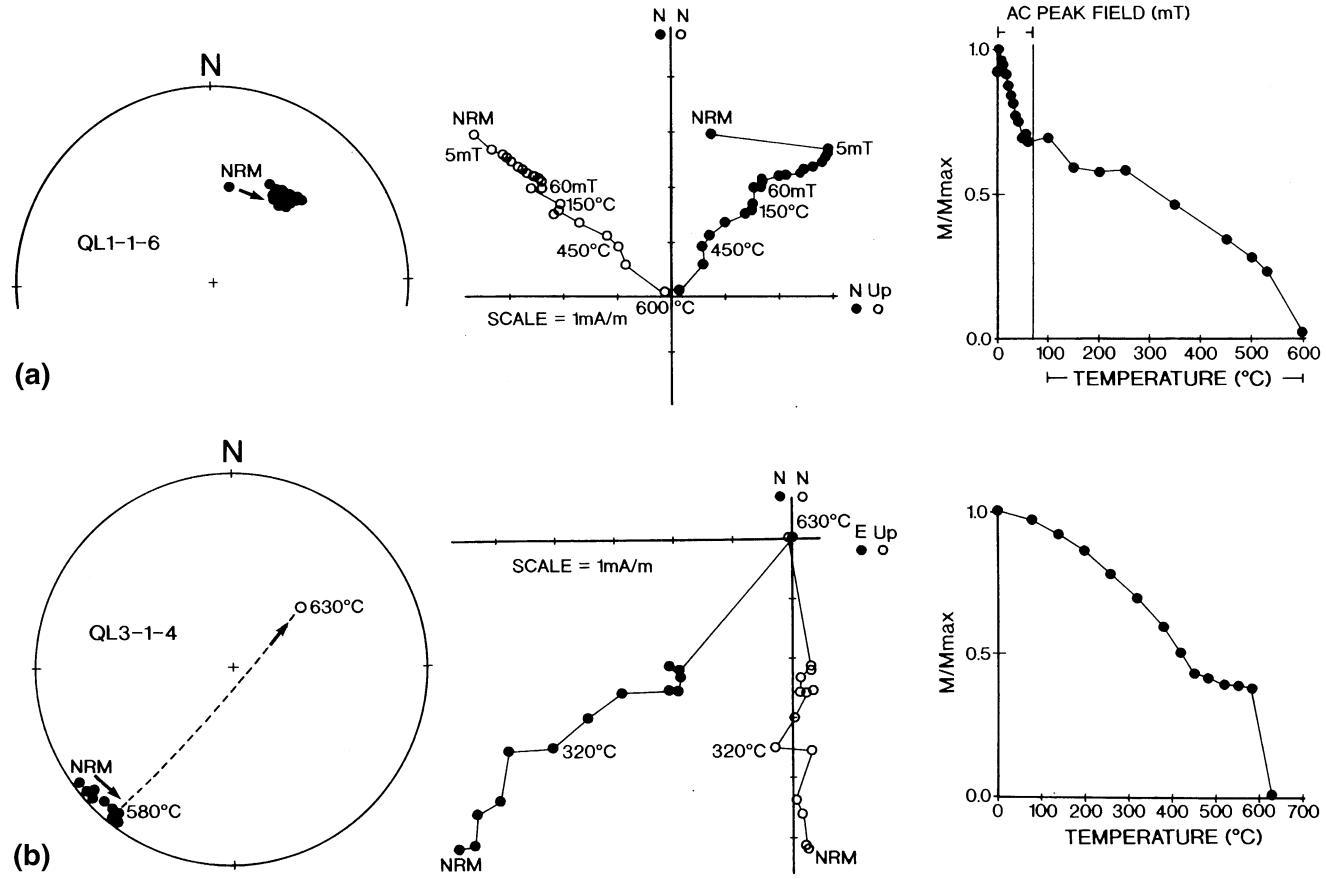

Figure 4. Orthogonal vector and equal-area projections of magnetization vectors (stratigraphic coordinates) for thermal and AF demagnetization and the corresponding normalized intensity decay curves are shown for two representative specimens: (a) QL1-1-6 (Querecual formation, 1.5 m from the Chimana/Querecual contact) and (b) QL3-1-4 (Querecual formation, 0.5 m from the Chimana/Querecual contact). Specimens were stepwise demagnetized using alternating fields (AF) up to 60 mT or thermally demagnetized from 50 °C (at about 50 °C increments) up to about 700 °C.

the gradual rise in the IRM acquisition curve for QL3-2 (Fig. 7c) suggests that high-coercivity phases such as goethite or haematite dominate this sample.

Thermal demagnetizations of composite IRMs in these samples reveal that the low- and intermediate-coercivity fractions of the IRMs are dominant in QL2-1 and QL3-4 (Figs 7a and b), whereas the high-coercivity fraction seems to be the most important IRM in QL3-2.

Low- and intermediate-coercivity IRMs for QL2-1 (Fig. 7a) and QL3-4 (Fig. 7b) decay progressively over a wide range of unblocking temperatures up to about 500 °C. This may be due to the presence of magnetite of different grain sizes as the dominant magnetic phase. Conversely, haematite seems to be the most important magnetic phase in QL3-2 (Fig. 7c).

Goethite, a magnetic mineral that commonly appears as a consequence of recent weathering and decomposition of iron-bearing minerals, seems also to be present in QL2-1 (Fig. 7a) and QL3-2 (Fig. 7c). The characteristic drop of all the composite IRMs at temperatures of about 150 °C reveals the presence of this mineral. Traces of additional magnetic phases such as pyrrhotite and maghemite may be present but do not appear to be important.

Although not entirely clear-cut, the behaviour of IRM acquisition and thermal demagnetization of composite IRMs seem to indicate a dominant presence of haematite in those sites that are closer to the contact (e.g. CL1-2 and QL3-2). A low-coercivity and intermediate-unblocking-temperature phase (e.g. magnetite) appears to be the chief magnetic mineral in those sites away (>4 m) from this lithological transition.

Electron microprobe analyses (EMPA) at 10 nA and 20 kV were made on a Querecual sample from site QL3-1 (~0.5 m from the contact). Quantitative analyses were impossible, largely due to small grain sizes and X-ray emission from surrounding carbonates. Grains of iron oxides are common in this sample. Back-scattered electron analyses (BSE) revealed the presence of two dominant chemistries for Fe-oxides. Most grains appeared homogeneous and showed a relatively dark (low atomic number) Z contrast. However, some grains showed regions of relatively light (higher atomic number) Z contrast. These heterogeneous grains have an irregular core of the lighter Z contrast partially enclosed by a rim of the dark Z contrast material. Quantitative analyses of FeO, SiO_2 and Al_2O_3 revealed that, in general, an increase in the Al content may be the cause of the darker Z contrast in the rims. The chemistry of the homogeneous grains, which showed relatively dark Z contrast under BSE, is very similar to the dark rim regions. However, totals for Fe suggest that the iron in the dark rim zones may be more oxidized.

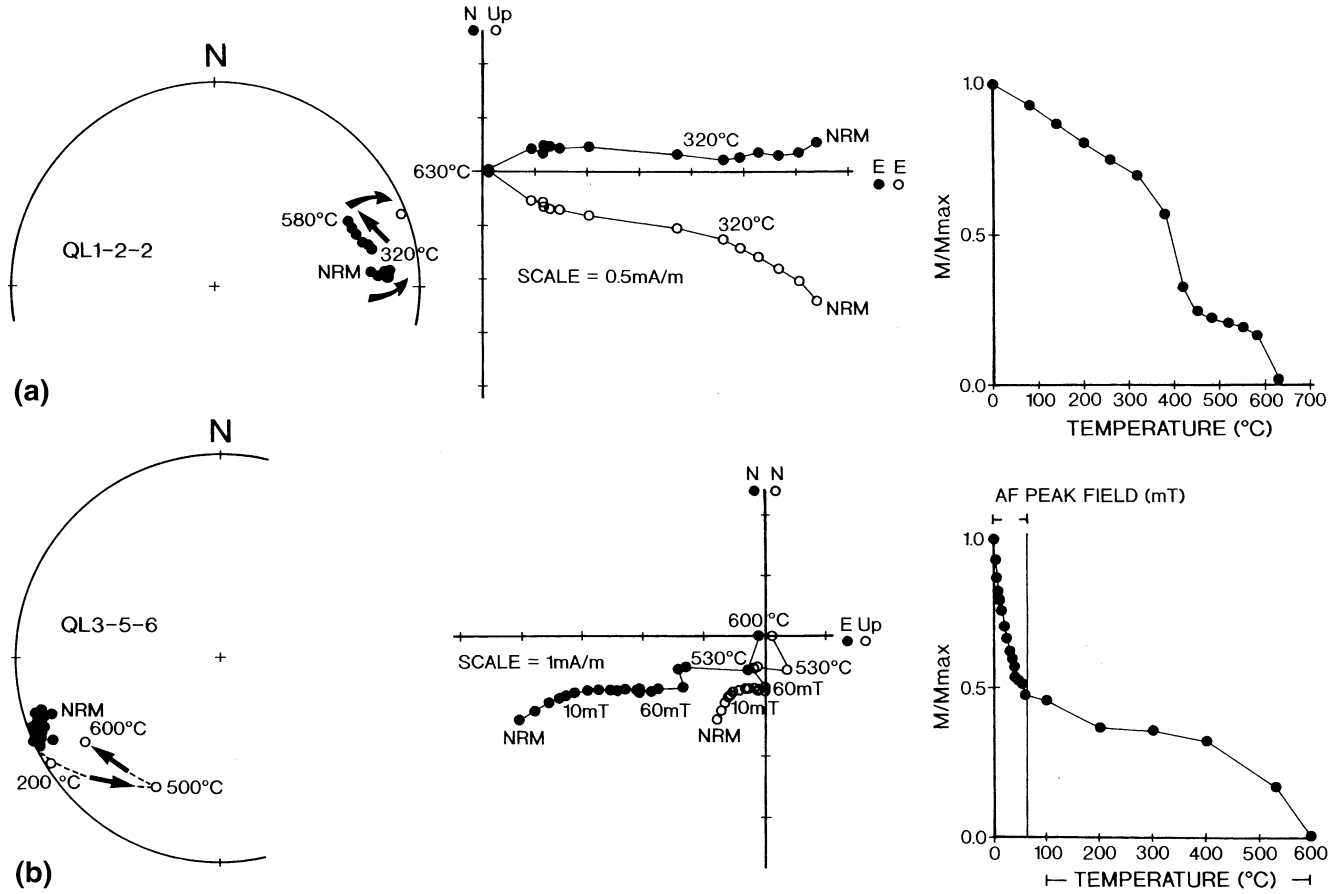

Figure 5. Orthogonal vector and equal-area projections of magnetization vectors (stratigraphic coordinates) for thermal and AF demagnetization and the corresponding normalized intensity decay curves are shown for two representative specimens: (a) QL1-2-2 (Querecual formation, 3.5 m from the Chimana/Querecual contact) and (b) QL3-5-6 (Querecual formation, 7.5 m from the Chimana/Querecual contact). Specimens were stepwise demagnetized using alternating fields (AF) up to 60 mT or thermally demagnetized from 50 °C (at about 50 °C increments) up to about 700 °C.

DISCUSSION

Thermochemical alteration around the Chimana/Querecual contact

Fig. 8(a) shows a profile of site-average NRM intensities for the high-coercivity (over 30 mT) and high-temperature (over 400 °C) components, along with their corresponding standard deviations (error bars), plotted against stratigraphic levels. Sites from all four sampled localities are included in this profile. A conspicuous peak roughly coincides with the contact itself, followed by a smaller high centred approximately 7.5 m away, within Querecual lithologies. We have previously suggested (Suárez *et al.* 1999 and Costanzo-Alvarez *et al.* 1999) that local alteration in the vicinity of the Chimana/Querecual formational transition could be characterized and 'mapped' by bulk magnetic properties (that is, initial susceptibility and site-averaged stable NRM intensity profiles such as the one in Fig. 8a). Site-averaged NRM intensity of the high-coercivity and high-unblocking-temperature components (Fig. 8a) are used here instead of site-averaged initial susceptibility data, since the latter could involve primary variations as well as non-magnetic contributions (e.g. ilmenite, biotite and hornblende).

Stratigraphic discontinuities, encompassed by the Chimana/Querecual contact, probably acted in the past as loci of chemical changes and local remagnetizations. Hence the observed pattern of these site-averaged stable NRM intensities suggests a possible causal relationship with the transition between the two lithologies. Harlan & Geissman (1989) have previously recognized remagnetizations of this kind that resulted from extensive hydrothermal alteration induced by migrating brines using unconformities as their flow areas millions of years after their deposition. They observed secondary NRMs in Precambrian rocks cropping out in close proximity to overlying Palaeozoic sediments (Colorado Front Range). For the particular case of the Chimana/Querecual contact, thermally stimulated depolarization (TSD) experiments have indicated the existence of water molecules bound to different sites in the material, whose abundance notably increases towards the contact (Suárez *et al.* 1999). This could be interpreted as a 'fossil record' of a hydrating event focused at the boundary between the two lithologies. Independent evidence for partial oxidation in samples from a Querecual site close to the contact (QL3-1) comes from electron microprobe analyses that reveal a haematite coating of the magnetite crystals. Moreover, palaeomagnetic and rock magnetic results seem to suggest

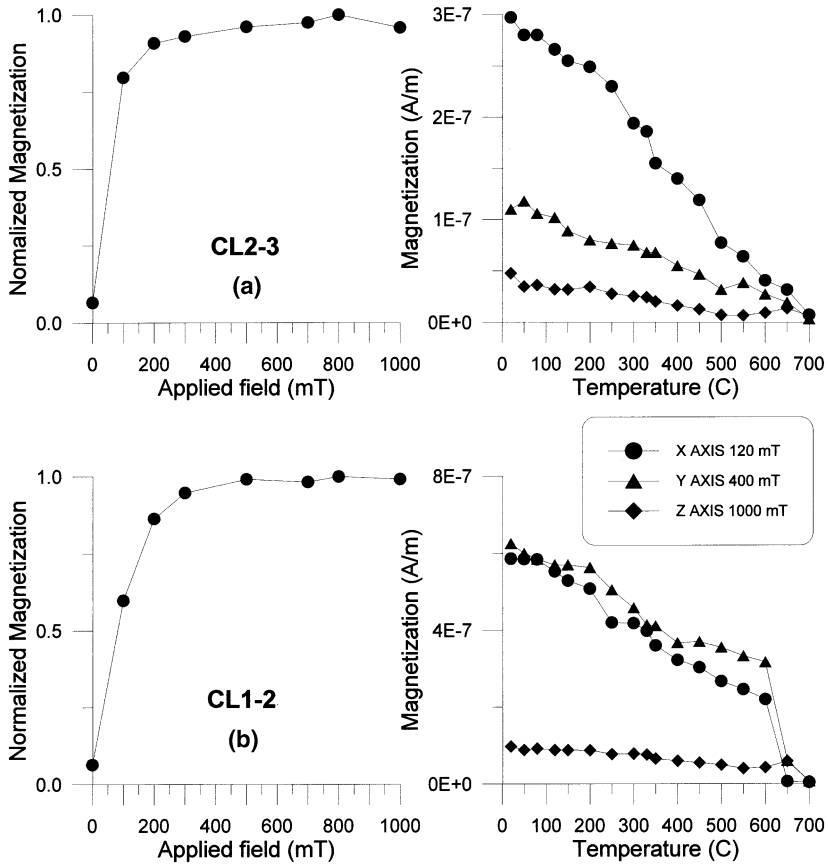

Figure 6. IRM acquisition curves and magnetic cleaning of composite IRMs (saturating fields: Z-axis = 1 T, Y-axis = 0.4 T, X-axis = 0.12 T) for representative samples: (a) CL2-3 (Chimana formation, −8 m from the Chimana/Querecual contact) and (b) CL1-2 (Chimana formation, −3.3 m from the Chimana/Querecual contact).

that haematite is an important magnetic phase in samples from those sites that lie closer to the lithological transition (Costanzo-Alvarez *et al.* 1999).

Most probably more than one remagnetization event affected the Albian/Cenomanian unconformity at the Pertigalete sections throughout its whole geological history. Thus, the profile of site-averaged NRM intensity of the high-coercivity and high-temperature components in Fig. 8(a) probably reflects overlapping thermochemical remagnetization events corresponding to at least two peaks of alteration. These events are centred at the contact itself and would be similar (but on a smaller scale) to those recognized elsewhere close to zones of weakness that have served as conduits for fluid circulation (e.g. Costanzo-Alvarez *et al.* 1993; Costanzo-Alvarez & Dunlop 1998). In those cases the 'thermochemical aureolae' have peaks of remagnetization at some distance from the foci of hydrothermal activity, displaying an ample range of overlapping directions of remanence, and followed by a gradual diminution of the state of alteration.

We suggest that by decoupling the most visible curves with the two prominent heights that appear to be superimposed on the site-averaged stable NRM intensity profiles (Querecual lithologies) of Fig. 8(a), it is possible to unravel part of the history of changing thermochemical conditions focused on the Chimana/Querecual unconformity. A method based on direct spectral analyses (DSA), previously proposed by Aldana *et al.* (1994), is used here as a preliminary approach to the study of the site-averaged stable NRM intensity profile of Fig. 8(a) for stratigraphic levels ranging between −5 and 25 m. Chimana sites at distances beyond −5 m are not taken into account in this analysis due to the dispersion observed between site-averaged stable NRM intensities and the within-site scatter of these values revealed by the large standard deviations (error bars in Fig. 8a). The experimental curve is approximated by the sum of N elementary Gaussian curves whose weights are adjusted by a non-linear regression least-squares method. The advantage of this procedure is that we do not have to make an *a priori* guess about the number of superimposed processes involved. The initial parameter set is the choice of the window on the stratigraphic level scale. This window is divided into N equally spaced bins for which the central value x_i is associated with the ith bin. The algorithm will return a histogram with the height of the contribution to the site-averaged stable NRM intensity curve of each elementary processes and thus the number of main events can be inferred.

DSA results reveal three overlapping curves in the Querecual lithologies and around the Chimana/Querecual contact (Fig. 8b). We find two major site-averaged stable NRM intensity peaks at −0.2 and 7.5 m from the lithological transition plus a minor one at about 15 m (Fig. 8b). Gaussian curves are perhaps not the best physical approach to the real shape of these peaks; however, they allow an unbiased identification of the main events that seem to overlap in this profile, as well as a satisfactory fit of a curve to the experimental data (Fig. 8c).

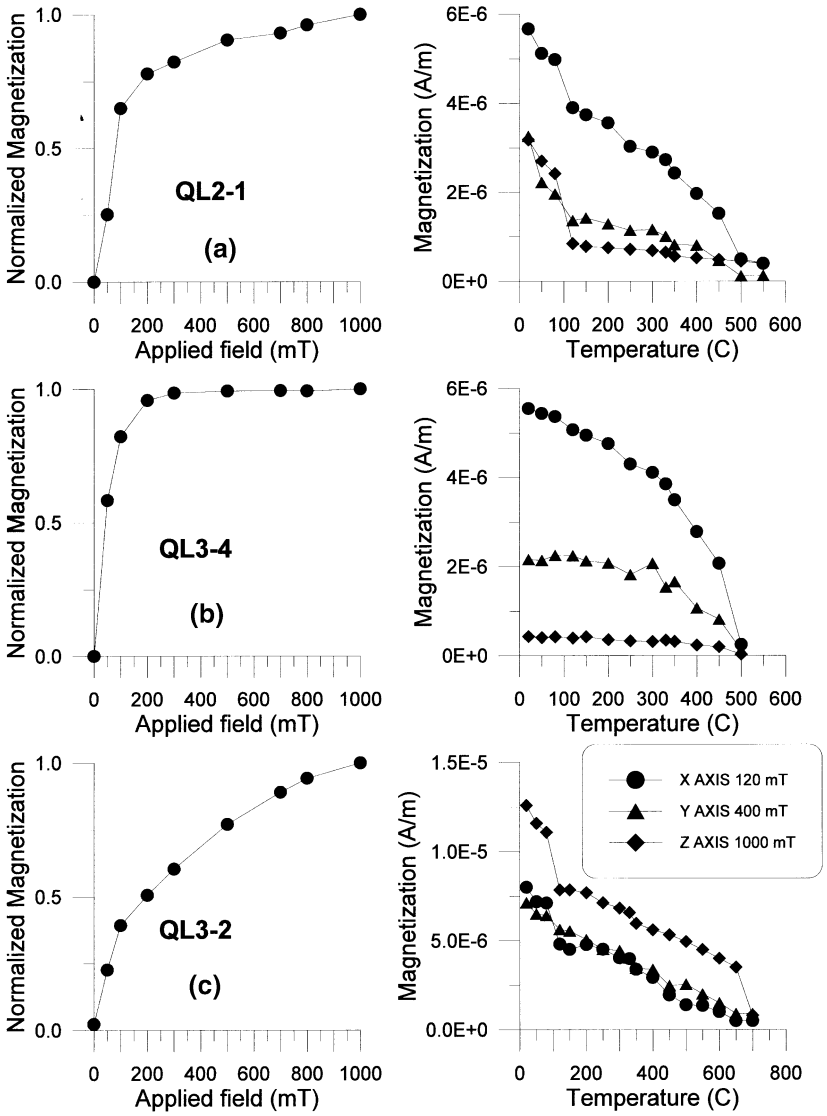

Figure 7. IRM acquisition curves and magnetic cleaning of composite IRMs (saturating fields: Z-axis = 1 T, Y-axis = 0.4 T, X-axis = 0.12 T) for representative samples: (a) QL2-1 (Querecual formation, 11.5 m from the Chimana/Querecual contact), (b) QL3-4 (Querecual formation, 7 m from the Chimana/Querecual contact) and (c) QL3-2 (Querecual formation, 4 m from the Chimana/Querecual contact).

An oxidizing event can decrease the effective grain sizes of multidomain magnetite via haematite coating. Costanzo-Alvarez *et al.* (1993) have previously pointed out that, as an overall consequence of such a process, an increase of the NRM values would be expected in those sites where this kind of alteration is more subdued (i.e. peak observed at -0.2 m from the contact). On the other hand, a reducing event such as the migration of hydrocarbons throughout porous rocks can also result in an NRM peak. In fact, it has been widely demonstrated (e.g. Machel 1996, 1995; Perroud *et al.* 1995; Robert & Turner 1993) that geochemical and microbial processes can dissolve haematite, with the consequent destruction of any primary magnetization and the reprecipitation of high-NRM minerals such as magnetite.

Patterns in site mean directions and their possible structural implications

Figs 9 shows equal-area projections of 24 site-mean directions of remanence for (a) tilted and (b) bedding-corrected magnetizations with coercivities over 30 mT and unblocking temperatures above 400 °C (Table 1). Site means have been calculated by using a combined analysis. Kirschvink mean directions (Kirschvink 1980) have been obtained for specimens with recognizable stable endpoints, and the intersection of remagnetization circles for specimens whose NRMs do not reach stable endpoints in the course of AF and thermal demagnetization (McFadden & McElhinny 1988).

For these site averages, α_{95} values range from 5° to 35°, and the Fisher precision k ranges from 5 to 144. The rather high α_{95} and low precisions reflect within-site dispersion due most probably to the effects of multiple and overlapping thermochemical remagnetization events that could have affected, to variable extents, individual samples from a single sedimentary horizon. Moreover, there is not a unique well-grouped palaeomagnetic component corresponding to a late remagnetization of these strata. Conversely, whereas inclination values range over a rather wide interval, there is also a noticeable streaking of site-mean declinations that suggests large differential rotations

Table 1. Palaeomagnetic results for Querecual and Chimana sites (around the upper Albian Chimana/Querecual contact) from the Pertigalete sedimentary sequence.

Site	Lithology	Distance to contact (m)	N	Geographic coordinates *In situ* Declination	Geographic coordinates *In situ* Inclination	Stratigraphic coordinates Tectonic correction Declination	Stratigraphic coordinates Tectonic correction Inclination	k	α_{95}
CL2-4	sandstone	−15	7	37	−12	40	−39	13	16
CL4-2	sandstone	−11	5	88.4	36	116	26	15	18.2
CL2-3	sandstone	−8	10	122	22	132	20.5	8	18.5
CL2-2	siltstone	−5	5	54	25	52.4	38.4	102	8.7
CL1-2	sandstone	−3.3	8	125	20	127	−10	12	18
CL4-1	siltstone	−2.2	5	90	0	67.4	−41	12	15
CL1-1	siltstone	−1.5	6	90.4	5.4	96	10	5	35
CL2-1	siltstone	−0.5	7	9	15	9	34	19	15
upper Albian Chimana/Querecual contact									
QL3-1*	limestone	0.5	7	226	9	226	−10	39	11
QL1-1*	limestone	1.5	8	46	20	62	36	12	17
QL4-1*	limestone	3.35	5	53	39	111	19	87	5.3
middle Albian									
QL1-2	limestone	3.5	7	75.5	23.4	89	21	6	30
QL4-2	limestone	3.80	10	62	45	109	37	144	5.4
QL3-2*	limestone	4	6	269.4	−11	273.6	−1.6	142	7.3
QL3-3	limestone	5.5	11	237	5	239	−10.4	16	12.2
QL3-4*	limestone	7	6	211	35	201.4	7	10	23
QL3-5	limestone	7.5	6	261	−3	265	−5.3	9	26
QL2-1	limestone	11.5	7	99	−32	73	−38	129	6.5
QL4-3	limestone	12	7	40	31	65	25.4	17	17
upper Cenomanian									
QL2-2*	limestone	16	5	67.4	−12	41	−14.3	31	17.3
QL4-4	limestone	17	7	46	−15	45	2.4	89	6.8
QL4-5	limestone	19	6	119	−24	104	−40	20	17
QL2-3*	limestone	20	9	94	−30	71	−34	16	14.4
QL2-4*	limestone	23	7	50	−33	37	−12	21	15

N is the number of specimens averaged per corresponding site; * represents the sites with biostratigraphic analyses.

around a vertical axis. We would expect, for northern Venezuela, average declinations and inclinations (D/I) ranging between 2°(182°)/12°(−12°) (Kl) and 9°(189°)/30°(−30°) (Tl) according to Cretaceous and Tertiary mean reference palaeopoles for South America (Van der Voo 1993). The actual geomagnetic field, for the geographical coordinates of our sampling location, has declination and inclination values around 10°/40° (Baldwin & Langel 1993).

In spite of the scatter of these directional data, Fig. 9 shows some groupings of site-mean directions that appear to spread at the NE–SE (Group A) and SW–NW (Group B) quadrants of the stereographs. Group B is restricted to sites from locality QL3 with declinations that seem to lie 180° apart from their Group A counterparts. A syntilting diagram (e.g. Schwartz & Van der Voo 1984) for these sets of data is pointless since the directional distributions involved in both untilted and tilted Groups A and B (Fig. 9) are clearly non-Fisherian ($k \approx 4$ in each case).

Various lines of evidence seem to indicate that the Chimana/Querecual contact has acted as a focus of alteration for its adjacent strata. However, it is not clear whether or not remagnetization of these sedimentary layers took place prior to major folding of the whole structure, hence the importance of assessing both untilted and tilted directions of remanence. In Fig. 10 we have plotted Group A and B site mean declinations against their corresponding stratigraphic levels for (a) 0 per cent and (b) 100 per cent untilting in order to check for a positional dependence of these data. The untilted profile of Fig. 10(b) improves to a certain extent the picture somehow concealed by its tilted counterpart (Fig. 10a). The general features that can be distinguished in this untilted profile are as follows:

(1) the minimum declination values are centred on the Chimana/Querecual transition;

(2) there are two progressive increases of declination values within the next 7.5 m of the Chimana and Querecual formations;

(3) there is a marginal decrease of declination values at the most distant sites (>7.5 m away from the contact) for both lithologies.

Moreover, it is noteworthy that site-averaged stable NRM intensity profiles (Fig. 8) seem to echo the main features of this untilted profile for both the Querecual lithologies and the Chimana strata adjacent to the contact. In fact, the two peaks of site-averaged stable NRM intensity values observed in Fig. 8(b) coincide approximately with a low and a peak of the declination values.

Although not conclusive, we suggest a possible integrated interpretation of these data. The presence of overlapping thermochemical remagnetization events, and their associated hybrid NRMs, could be inferred as the main reasons not only for within-site dispersion, but also for the gradual variation of site mean declinations observed in Fig. 10(b). In fact, minimum

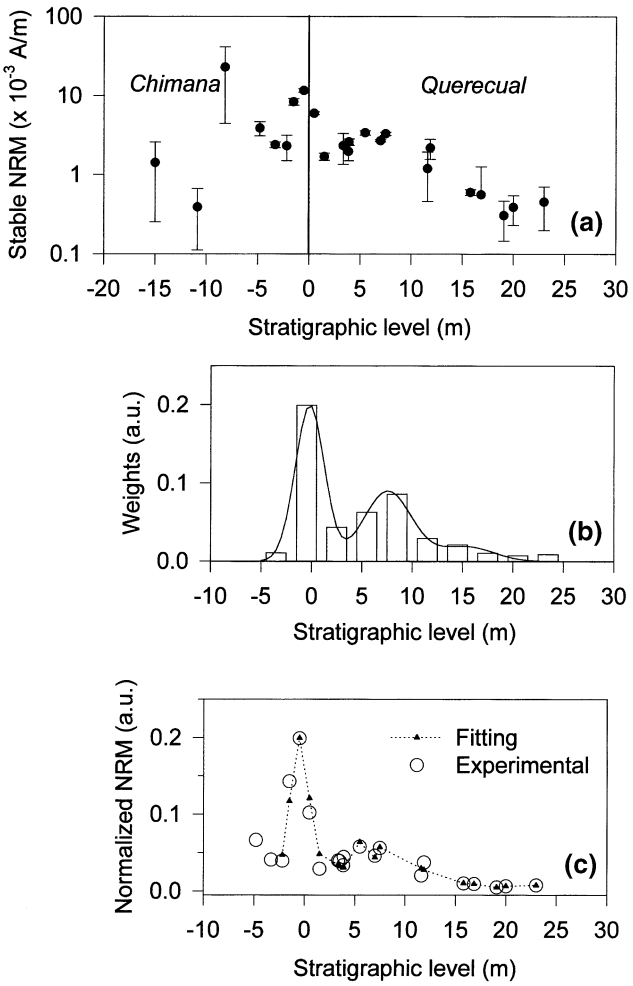

Figure 8. Analysis of overlapping remagnetization events around the Chimana/Querecual contact. (a) Profile of site-averaged intensity of the high-coercivity (over 30 mT) and high-temperature (over 400 °C) components versus stratigraphic level. Sites from all four localities sampled are included. Error bars are the corresponding site-averaged standard deviations. (b) Direct spectral analyses (DSA) on the site-averaged stable NRM intensity profile. The experimental curve is approximated by the sum of N elementary Gaussian curves whose weights are adjusted by a non-linear regression least-squares method. The initial parameter set is the choice of the window on the stratigraphic level scale. This window is divided into N equally spaced bins for which the central value x_i is associated with the ith bin. The algorithm returns a histogram with the height of the contribution to the site-averaged stable NRM intensity curve of each elementary processes and thus the number of overlapping events can be inferred. (c) Fitting of a computed curve to the experimental data after DSA. Site-averaged stable NRM intensities for Chimana sites at distances over 5 m from the contact are not taken into account due to the dispersion observed between site-averaged stable NRM intensities, plus the within-site scatter of these values revealed by the large standard deviations. In (b) and (c), a.u. stands for arbitrary units.

declinations could have been recorded as a consequence of a late remagnetization event that post-dated major horizontal rotations of the whole structure and reactivated the contact, hence their proximity to the declinations expected for late Cretaceous and Tertiary northern South America ($\sim 10^\circ$). As we move away from the focus of late alteration the older rotated overprints are obliterated to varying degrees by their younger and less rotated counterparts. Therefore, at least two distinct remanences must be mixed at the site and sample levels. The problems we have encountered in separating different NRMs in a single specimen (i.e. within-site dispersion) by routine AF and thermal demagnetizations (e.g. Figures 3, 4 and 5) could be due, in part, to the thermochemical origin of these components, which would result in a substantial overlap of coercivity and unblocking temperature spectra.

We have failed to explain the results of Group B at sampling locality QL3 in a satisfactory manner. However, site-averaged stable NRM intensity and declination results for these sites (Figs 8 and 10) roughly fit the general trends of the rest of the data for other sampling localities, suggesting that these remanences could record similar remagnetization events. This would imply that the peaks of late alteration recorded at QL1, 2 and 4 were perhaps diachronous with respect to QL3.

A tentative and simplified reconstruction of the possible chain of thermal and tectonic events that could have led to the present-day palaeomagnetic and rock magnetic evidence is sketched in Fig. 11. The 'thermochemical curves', depicting only two of the remagnetization peaks (E1 and E2) that have affected this formation in the past, are based on the main signals separated by DSA from the site-averaged stable NRM intensity profile of Fig. 8(a). In order to simplify this model, the third peak about 15 m from the contact has been assumed here as a marginal extension of E2.

Fig. 11(a) describes the initial remagnetization of the sequence (declinations approximately 10°) as a consequence of E1, which peaks approximately 7.5 m away from the contact. Fig. 11(b) illustrates the shift of these same declinations, after a clockwise horizontal rotation of approximately 80°–100° with respect to the geographical north, that has taken place around a vertical axis. Finally, Fig. 11(c) displays the actual situation with an overlapping remagnetization event (E2) whose maximum lies, within Chimana, in the vicinity of the contact itself. Therefore, a possible interpretation of the positional dependence of declination values observed in Fig. 10(b) could be as follows:

(1) sites over the contact, where the peak of the latest remagnetization event is more conspicuous, are the ones with less rotated declinations (at -0.2 m with declinations approximately 10°);

(2) sites at about 7.5 m from the contact, where the peak of the first remagnetization event is more conspicuous, are the ones with maximum declination rotations (approximately between 80° and 100° with respect to N and S for Groups A and B, respectively);

(3) the rest of the sites, located away from the two remagnetization peaks (i.e. between 0 and 7.5 m or beyond 7.5 m from the contact) have hybrid declinations.

Since there is no direct way of determining the absolute ages at which these tectonic and remagnetization events took place, their position in the geological setting of post-Cretaceous Venezuela is debatable. However, from the discussion above it becomes clear that it is possible to unravel to some extent the sequence of their relative occurrence times.

One of the most important post-Cretaceous events in eastern Venezuela, associated with a reducing environment and thus with the ensuing formation of high-NRM diagenetic magnetic minerals (e.g. magnetite), is that related to oil and gas generation from the source rocks of the Querecual formation.

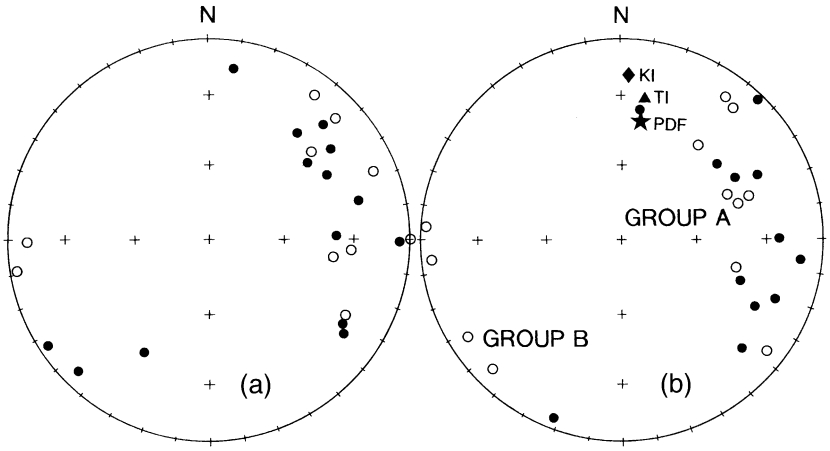

Figure 9. Equal-area projections of site means calculated using a combined analysis (McFadden & McElhinny 1988) that includes the Kirschvink mean directions (Kirschvink 1980) for specimens with recognizable stable endpoints and the intersection of remagnetization circles for specimens whose NRMs do not reach stable endpoints in the course of AF and thermal demagnetization. These site means are shown in (a) geographical and (b) stratigraphic coordinates. Group A refers to site means from localities 1, 2 and 4. Group B is restricted to site means from locality 3. Also in (b) Cretaceous (diamond, Kl) and Tertiary (triangle, Tl) mean reference palaeopoles for South America (Van der Voo 1993) are shown along with the present dipolar field (star, PDF) for the geographical coordinates of our sampling location (Baldwin & Langel 1993).

The thermal history of these rocks has been reconstructed by analyses of vitrinite reflectance (Talukdar *et al.* 1988; Gallango & Parnaud 1995). These studies suggest that this formation reached the oil window before the middle Miocene, attaining temperatures close to 350 °C, with R_0 ranging between 1.3 and 2 (Talukdar *et al.* 1988; Gallango & Parnaud 1995). It is quite unlikely that any previous magnetic remanence carried by these rocks could survive such a major thermochemical peak. Although pre-Miocene magnetite could have been a stable magnetic phase in reducing conditions (Machel 1996, 1995), their primary NRMs would not survive a prolonged heating in nature (i.e. 10^5–10^7 years) of ~350 °C. In fact, 350 °C is equivalent to laboratory unblocking temperatures higher than 450 °C (Pullaiah *et al.* 1975).

On the other hand, analyses of South Atlantic magnetic anomalies (Ladd 1976) seem to indicate that during late Tertiary times South America moved northwards with respect to North America. According to Ladd (1976), such a relative motion is related to the compressive tectonic regime on the northern and southern boundaries of the Caribbean plate and may have been responsible for late Eocene to Miocene folding in northern Venezuela. In fact, geological evidence suggests that after uplift and gravity sliding the Caribbean Range was compressed by NNW–SSE forces from early Eocene to Miocene times (e.g. Bell 1972; Harvey 1972; Santamaria & Schubert 1974). This compression gave rise to the widespread N70–80E-striking geological structures that have been recognized in northeastern Venezuela (rather easterly striking structures in the vicinity of Pertigalete according to the geological evidence shown in Fig. 1). Moreover, Metz (1964) has found that the time of folding and thrusting near the El Pilar fault zone (Fig. 1) and Pertigalete was between post-Eocene and Pliocene times. Thus, although somewhat conjectural, it seems reasonable to believe that the series of events summarized in Fig. 11, bracketed between a conspicuous reducing event (E1?) and perhaps a major folding of the Pertigalete strata (Fig. 10), occurred within the period encompassed by middle Miocene and Pliocene times.

CONCLUSIONS

(1) An upper Albian age has been determined, on biostratigraphic grounds, for the formational Chimana/Querecual contact of the Pertigalete sedimentary sequence (Pertigalete cement quarry, northeastern Venezuela).

(2) Palaeomagnetic and rock magnetic results indicate that the main magnetic mineralogies and chief carriers of most stable NRMs in these rocks are fine-grained magnetite and haematite.

(3) We suggest that local alteration in the vicinity of the Chimana/Querecual contact may be 'mapped' by a profile of site-averaged stable NRM intensities, the probable outcome of overlapping and diachronous thermochemical events. Direct spectral analyses performed on this profile, within Querecual lithologies, allow the separation of three major signals that probably correspond to two events of thermochemical alteration.

(4) Palaeomagnetic results show a considerable streaking of site-mean declinations, suggesting that tectonic or structural horizontal rotations around a vertical axis occurred after NRM acquisition.

(5) Horizontal rotation angles have been plotted against stratigraphic levels for both tilted and bedding-corrected declinations. Some trends of these data can be distinguished in the bedding-corrected profile. At the same time, site-averaged stable NRM intensity profiles seem to echo the main features of this bedding-corrected profile for the Querecual lithologies and the Chimana strata adjacent to the contact. This type of correlation between alteration events and declination values suggests that thermochemical remagnetizations are perhaps responsible not only for within-site dispersion but also for the gradual variation of hybrid site mean declinations.

(6) We propose a simplified three-stage reconstruction of the possible chain of thermal and tectonic events that could lead to the present-day palaeomagnetic and rock magnetic evidence: (i) an initial remagnetization of the sequence as a consequence of E1; (ii) a shift of these same declinations after

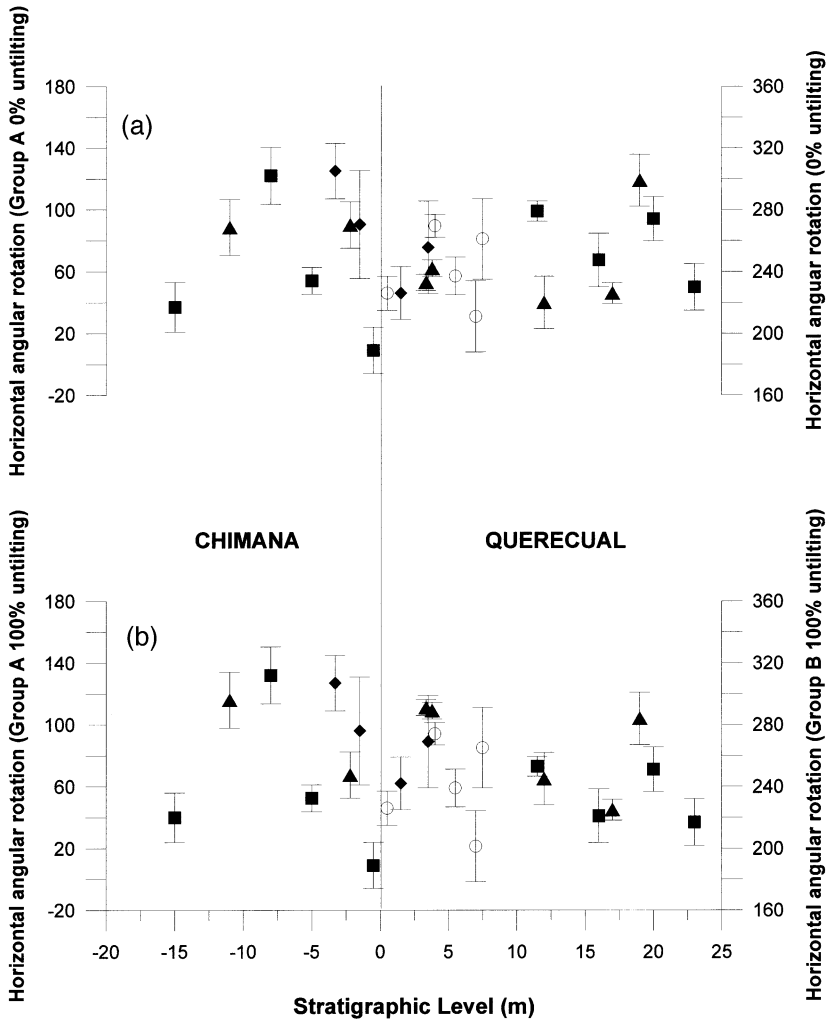

Figure 10. Profiles of declination versus stratigraphic level for (a) 0 per cent untilting and (b) 100 per cent untilting. Different symbols represent the different localities sampled: diamonds = L1, squares = L2, circles = L3 (Group B) and triangles = L4. Solid symbols are declinations between 0° and 180° (Group A horizontal rotations with respect to the geographical north), whereas open symbols represent declinations between 180° and 360° (Group B horizontal rotations with respect to the geographical south). The origin is taken at the Chimana/Querecual contact. Positive stratigraphic levels (in metres) correspond to Querecual horizons and negative stratigraphic levels to Chimana horizons. Error bars are α_{95} values shown in Table 1.

a clockwise horizontal rotation around a vertical axis of approximately 80° to 100° with respect to the geographical north and south for Groups A and B, respectively; and (iii) the actual situation with an overlapping remagnetization event (E2) whose maximum lies, within Chimana, at approximately 0.2 m from the contact.

(7) There is no direct way of determining the age bracket in which these events took place. However, it is quite unlikely that any primary magnetic remanence in these rocks survived the major thermochemical event associated with oil and gas generation from the source rocks of the Querecual formation (peak temperatures approximately 350 °C) that took place before middle Miocene times. On the other hand, there is widespread evidence for geological structures striking N70–80E in northeastern Venezuela (easterly striking around Pertigalete according to the structural evidence presented in Fig. 1), probably induced by the NNW–SSE push of South America towards the southern boundary of the Caribbean plate during late Tertiary times. In fact, the period of major folding and thrusting near the El Pilar fault zone and the Pertigalete region has been determined by geological evidence to be between post-Eocene and Pliocene times (Metz 1964). Therefore, it seems reasonable to believe that the series of thermochemical and tectonic events proposed in our model in Fig. 11 took place between the middle Miocene and Pliocene.

ACKNOWLEDGMENTS

We would like to thank Amarilis de Calzadilla (Vencemos, Pto. la Cruz), Francia Galea (PDVSA) and Humberto Carvajal Chitty (INTEVEP S.A.) for logistic support in the field and geological hints during the sampling of the Pertigalete sequence in eastern Venezuela. Max Furrer (PDVSA) performed the foraminiferal dating of the Pertigalete samples. Angela Doak and Allan Jones (University of Edinburgh) performed some of the AF and thermal demagnetizations, as well as NRM measurements and the IRM experiments of the samples used in this paper. Trevor Williams (University of Edinburgh) and

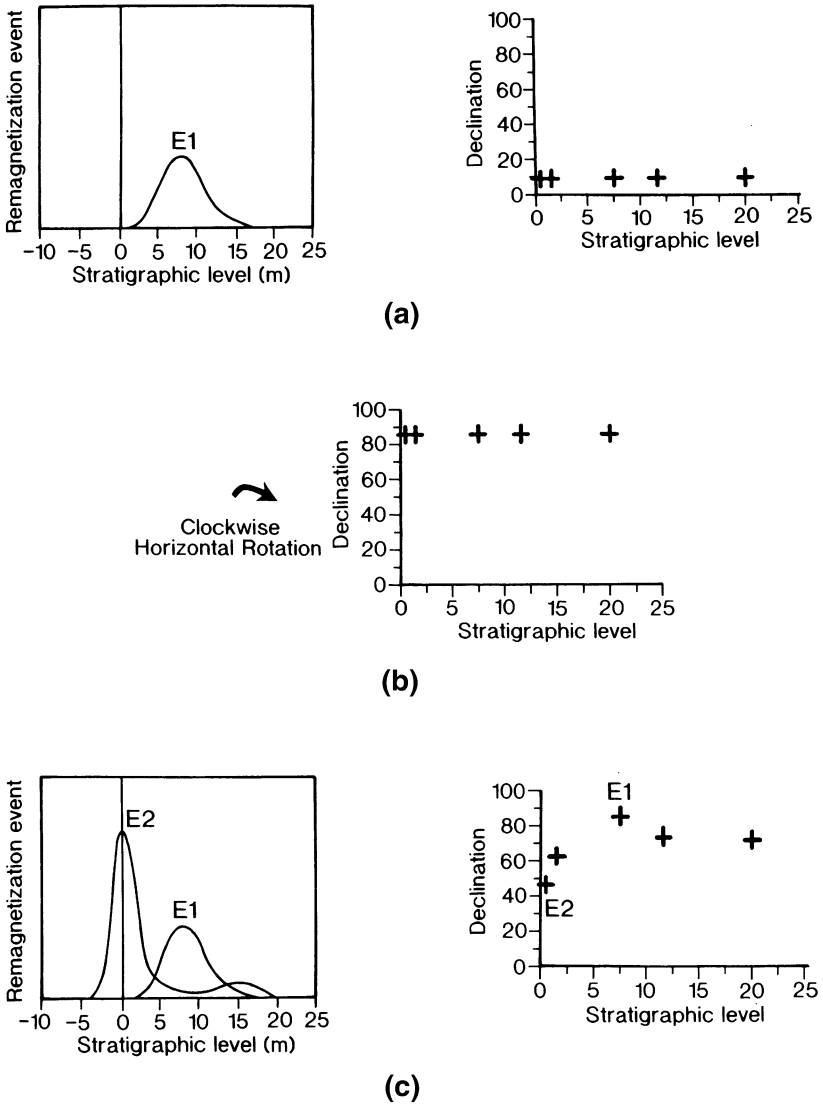

Figure 11. Sketch of our proposed sequence of thermal and tectonic events leading to present-day palaeomagnetic and rock magnetic evidence. (a) Initial remagnetization of the strata as a consequence of E1. (b) Shift of these same declinations after a clockwise horizontal rotation around a vertical axis approximately between 80° and 100° (with respect to the geographical north and south for Groups A and B, respectively). (c) Actual situation with an overlapping remagnetization event (E2). The 'thermochemical curves' depicting the remagnetization peaks are based on the main signals separated by DSA from the site-averaged stable NRM intensity profile of Fig. 8(a).

Jose Luis Gago (Universidad Simón Bolívar) also assisted us in the laboratory measurements. The software used for processing and interpreting the palaeomagnetic data was created and generously provided by Randolph Enkin (Geological Survey of Canada, Sidney BC, Canada). Valuable comments on a preliminary version of this paper by Randy Enkin were very much appreciated as well as thoughtful reviews by Peter Turner and an anonymous referee. This work has been funded by the British Council of Venezuela and the Decanato de Investigaciones (Universidad Simón Bolívar).

REFERENCES

Aldana, M., Laredo, E., Bello, A. & Suárez, N., 1994. Direct signal analysis applied to the determination of the relaxation parameters from TSDC spectra of polymers, *J. Polym. Sci.,* B, **32,** 2197–2206.

Baldwin, R.T. & Langel, R., 1993. Tables and Maps of the DGRF 1985 and IGRF 1990, *IAGA Bull.,* **54,** 117.

Bell, J.S., 1972. Tectonic evolution of the central part of the Venezuelan coast ranges, in *Caribbean Geophysical Tectonics and Petrologic Studies,* ed. Donnelly, T.W., *Geol. Soc. Am. Mem.,* **130,** 107–118.

Burmester, R.F., Beck, M.E., Speed, R.C. & Snoke, A.W., 1996. A preliminary paleomagnetic pole for mid-Cretaceous rocks from Tobago: further evidence for large clockwise rotations in the Caribbean-South American plate boundary zone, *Earth planet. Sci. Lett.,* **139,** 79–90.

Costanzo-Alvarez, V. & Dunlop, D.J., 1998. A regional paleomagnetic study of lithotectonic domains in the Central Gneiss Belt, Grenville Province, Ontario, *Earth planet. Sci. Lett.,* **157,** 89–103.

Costanzo-Alvarez, V., Dunlop, D.J. & Pesonen, L.J., 1993. Paleomagnetism of alkaline complexes and remagnetization in the Kapuskasing structural zone, Ontario, Canada, *J. geophys. Res.,* **98** (B3), 4063–4079.

Costanzo-Alvarez, V., Aldana, M., Suárez, N., Gago, J.L. & Williams, W., 1999. Rock magnetic and dielectric characterizations of a formational contact in Cretaceous strata (eastern Venezuela), *Phys. Chem. Earth,* **24,** 763–771.

Duncan, R.A. & Hargraves, R.B., 1984. Plate tectonic evolution of the Caribbean region in the mantle reference frame, *Geol. Soc. Am. Mem.,* **162,** 81–93.

Gallango, O. & Parnaud, F., 1995. Two-dimensional computer modeling of oil generation and migration in a transect of the eastern Venezuela basin, in *Petroleum Basins of SouthAmerica,* eds Tankard, A.J., Suarez, R. & Welsik, H.J., *AAPG Mem.,* **62,** 727–740.

Gonzalez de Juana, C., Iturralde de Arozena, J.M. & Picard, C., 1980. *Geología de Venezuela y de sus cuencas petrolíferas,* Foninves, Caracas, Venezuela.

Harlan, S.S. & Geissman, J.W., 1989. Late Paleozoic remagnetization of Proterozoic crystalline rocks, Colorado Front Range, Colorado, *EOS, Trans. Am. geophys. Un.,* **70,** 311.

Harland, W.B., Armstrong, R.L., Cox, A.V., Craig, L.E., Smith, A.G. & Smith, D.G., 1990. *A Geologic Time Scale 1989,* Cambridge University Press, Cambridge.

Harvey, S.R.M., 1972. Origin of southern Caribbean Mountains, in *Studies in Earth and Space Sciences,* ed. Shagam, R., *Geol. Soc. Am. Mem.,* **132,** 387–400.

Kirschvink, J.L., 1980. The least-squares line and plane and the analysis of paleomagnetic data, *Geophys. J. R. astr. Soc.,* **62,** 699–718.

Ladd, J.W., 1976. Relative motion of South America with respect to North America and Caribbean tectonics, *Geol. Soc. Am. Bull.,* **87,** 969–976.

Lowrie, W., 1990. Identification of ferromagnetic minerals in a rock by coercivity and unblocking temperature properties, *Geophys. Res. Lett.,* **17,** 159–162.

MacDonald, W.D., 1980. Anomalous paleomagnetic directions in late Tertiary andesitic intrusions of the Cauca depression, Colombian Andes, *Tectonophysics,* **68,** 339–348.

MacDonald, W.D., 1990. Survey of Caribbean paleomagnetism, in *The Geology of North America, Vol. H: The Caribbean Region,* pp. 393–404, eds Dengo, G. & Case, J., Geol. Soc. Am., Boulder, CO.

MacDonald, W.D. & Van Horn, J., 1977. Paleomagnetism of the Haw's Bill Formation, Tobago, in *Memoria, Congreso Geologico Venezolano V,* Vol. 2, pp. 817–834, Ministerio de Enrgia y Minas, Venezuela.

Machel, H.G., 1995. Magnetic mineral assemblages and magnetic contrasts in diagenetic environments with implications for studies of paleomagnetism, hydrocarbon migration and exploration, in *Paleomagnetic Applications in Hydrocarbon Exploration and Production,* eds Turner, P. & Turner, A., *Geol. Soc. Spec. Publ.,* **98,** 9–29.

Machel, H.G., 1996. Magnetic contrasts as result of hydrocarbon seepage and migration, in *Hydrocarbon Migration and its Near-Surface Expression,* eds Schumacher, D. & Abrams, M.A., *AAPG Mem.,* **66,** 99–109.

Maze, W.B. & Hargraves, R.B., 1984. Paleomagnetic Results of the Jurassic La Quinta Formation in the Perija Range, Venezuela and their tectonic significance, *Geol. Soc. Am. Mem.,* **162,** 287–293.

McClelland-Brown, E., 1982. Discrimination of TRM and CRM by blocking-temperature spectrum analysis, *Phys. Earth planet. Inter.,* **30,** 405–414.

McFadden, P.L. & McElhinny, M.W., 1988. The combined analysis of remagnetization circles and direct observations in palaeomagnetism, *Earth planet. Sci. Lett.,* **87,** 161–172.

Metz, H., 1964. Geology of the El Pilar fault zone, state of Sucre, Venezuela, *PhD thesis,* Princeton University, Princeton.

Passalacqua, H., Fernández, F., Gou, Y. & Roure, F., 1995. Crustal architecture and strain partitioning in the eastern Venezuelan Ranges, in *Petroleum Basins of South America,* eds Tankard, A.J., Suárez, R. & Welsink, H.J., *AAPG Mem.,* **62,** 667–679.

Perarnau, A., 1985. Paleomagnetic Studies of some Venezuelan rocks, *PhD thesis,* University of Newcastle, Newcastle-upon-Tyne.

Perroud, H., Chauvin, A. & Rebelle, M., 1995. Hydrocarbon seepage through chemical remagnetization, in *Paleomagnetic Applications in Hydrocarbon Exploration and Production,* eds Turner, P. & Turner, A., *Geol. Soc. Spec. Publ.,* **98,** 33–41.

Pullaiah, G., Irving, E., Buchan, K.L. & Dunlop, D.J., 1975. Magnetization changes caused by burial and uplift, *Earth planet. Sci. Lett.,* **28,** 133–143.

Roberts, A.P. & Turner, G.M., 1993. Diagenetic formation of ferromagnetic iron sulphide minerals in rapidily deposited marine sediments, South Island, New Zeland, *Earth planet. Sci. Lett.,* **115,** 257–273.

Santamaría, F. & Schubert, C., 1974. Geochemistry and geochronology of the southern Caribbean-northern Venezuela plate boundary, *Geol. Soc. Am. Bull.,* **85,** 1085–1098.

Schwartz, S. & Van der Voo, R., 1984. Paleomagnetic study of thrust sheet rotation during foreland impingement in the Wyoming-Idaho overthrust belt, *J. geophys Res.,* **89**(B12), 10 077–10 086.

Skerlec, G.M. & Hargraves, R.B., 1980. Tectonic significance of paleomagnetic data from northern Venezuela, *J. geophys. Res.,* **85,** 5303–5315.

Stearns, C., Mauk, F.J. & Van der Voo, R., 1982. Late Cretaceous—Early Tertiary paleomagnetism of Aruba and Bonaire (Netherlands Leeward Antilles), *J. geophys. Res.,* **87,** 1127–1141.

Suárez, N., Aldana, M. & Costanzo-Alvarez, V., 1999. TSDC study of a sedimentary sequence in northeastern Venezuela, *Radiation Effects Defects Solids,* **51,** 57–63.

Talukdar, S., Gallango, O. & Ruggiero, A., 1988. Generation and migration of oil in the Maturin Subbasin, Eastern Venezuela Basin, *Org. Geochem.,* **13,** 537–547.

Van der Voo, R., 1993. *Paleomagnetism of the Atlantic, Tethys and Iapetus Oceans,* Cambridge University Press, Cambridge.

Vivas, V. & Macsotay, O., 1995. Dominios tectono-estratigráficos del Cretácico Neogeno en Venezuela Nor-oriental, *IX Congreso Latinoamericano de Geología,* Caracas, Venezuela.